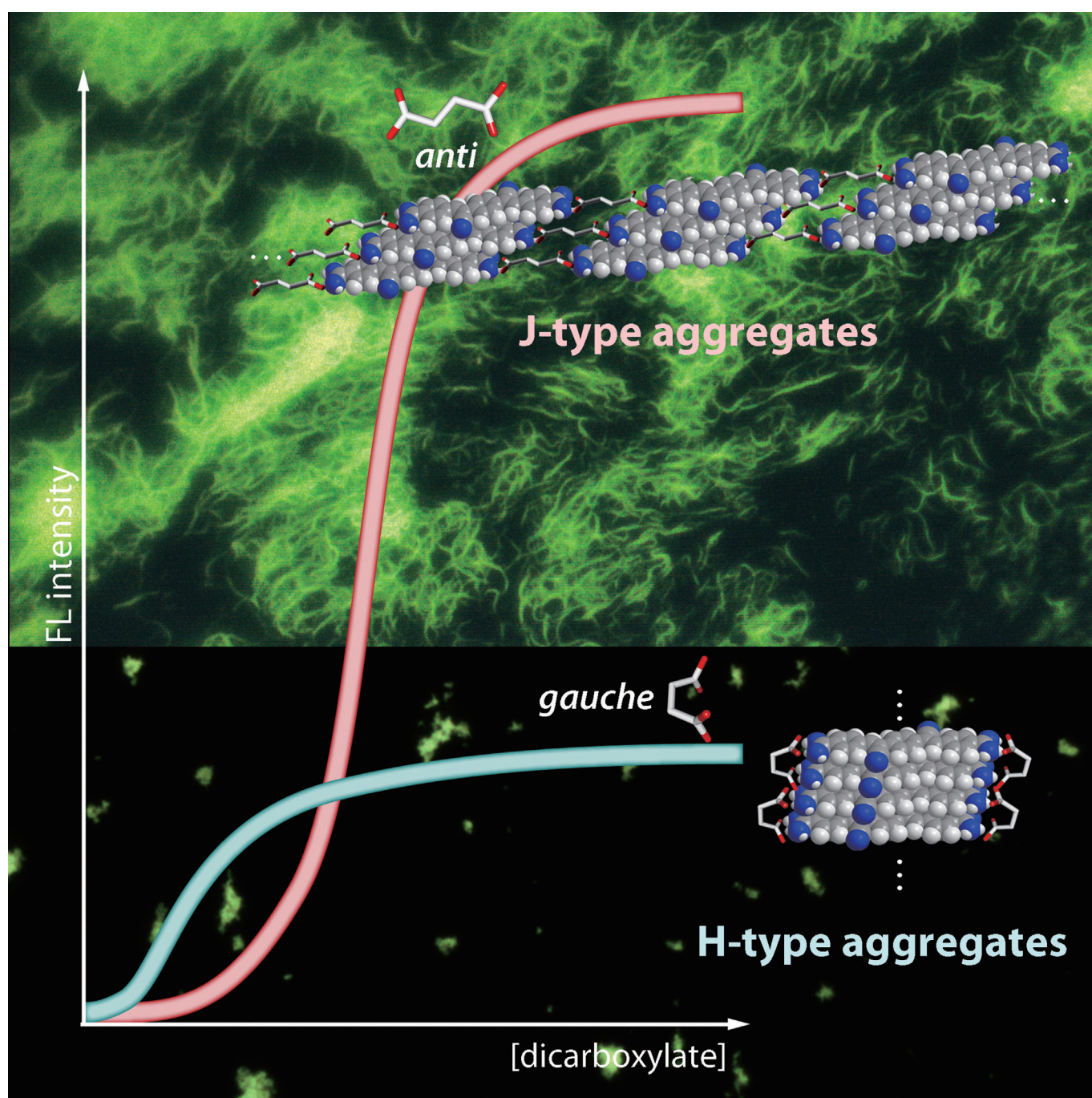


Fluorescent Chemosensors

Translation of Dicarboxylate Structural Information to Fluorometric Optical Signals through Self-Assembly of Guanidinium-Tethered Oligophenylenevinylene

Takao Noguchi,^{*,[a, b]} Bappaditya Roy,^[a] Daisuke Yoshihara,^[b] Youichi Tsuchiya,^[b] Tatsuhiro Yamamoto,^[b] and Seiji Shinkai^{*,[a, b, c]}

Abstract: Although self-assembly has realized the spontaneous formation of nanoarchitectures, the nanoscopic expression of chemical structural information at the molecular level can alternatively be regarded as a tool to translate molecular structural information with high precision. We have found that a newly developed guanidinium-tethered oligophenylenevinylene exhibits characteristic fluorescence (FL) responses toward L- and meso-tartarate, wherein the different self-assembly modes, termed J- or H-type aggregation, are directed according to the molecular information encoded as the chemical structure. This morphological difference originates

from the geometric *anti* versus *gauche* conformational difference between L- and meso-tartarate. A similar morphological difference can be reproduced with the geometric C=C bond difference between fumarate and maleate. In the present system, the dicarboxylate structural information is embodied in the inherent threshold concentration of the FL response, the signal-to-noise ratio, and the maximum FL wavelength. These results indicate that self-assembly is meticulous enough to sense subtle differences in molecular information and thus demonstrate the potential ability of self-assembly for the expression of a FL sensory system.

Introduction

By applying the fundamental principles and methodologies of supramolecular chemistry,^[1] a wide variety of molecules have been designed and self-assembled into well-ordered nanoarchitectures to create soft materials with sophisticated functions.^[2–9] In the chromophoric self-assemblies, for example, the relative arrangements of chromophores, termed J and H type, predetermine the photophysical phenomena^[10,11] and thus result in optoelectronic materials with unique light-harvesting, energy/charge-transporting, and light-emitting properties.^[12–15] The exploitation of such properties is one of the reasons why the relationship between the molecular structure and its self-assembly morphology has long been studied through appropriate molecular design. From this context, self-assembly has been recognized as a tool to realize the spontaneous formation of functional nanoarchitectures. Therein, a small change in the molecular structure fatefully alters the resulting self-assembly structure. For example, Oda et al. reported that twisted multilamellar superstructures are formed by the self-assembly of a gemini surfactant in the presence of L-tartarate as a counterion, whereas the molecule lacking one hydroxy group, that is, the L-malate anion, generates flat bilayer structures.^[16] Fujita and co-workers described how the structure of multicomponent coordination polyhedra self-assembled from metal ions and bridging ligands is determined critically by the ligand bent

angle.^[17] Yagai et al. also demonstrated that characteristic nanoarchitectures consisting of rings and rods are formed by just regioisomerism in self-assembling naphthalene chromophores.^[18] These studies clearly exemplify that self-assembly is able to amplify a subtle difference in the molecular structure (information) into a big difference in the resulting self-assembled structure (output). Thus, one can regard self-assembly as a function to convert information programmed as a molecular structure into a superstructure output.

In this case, when a characteristic fluorescence (FL) signaling is achieved as an output of self-assembly through interaction with the concerned target, the FL signaling will reflect detailed structural information about the target molecule. This process is fundamentally regarded to be a translation of molecular structural information into FL through self-assembly. In this context, such an assembly-based system is intrinsically different from the conventional sensory system based on molecular recognition through receptor–guest binding.^[19] To the best of our knowledge, the application of self-assembly to a FL sensory system has rarely been explored, in spite of its potential ability to read out molecular information.^[20]

In order to realize a synergistic marriage of self-assembly and FL sensing, we have focused on aggregation-induced emission (AIE).^[21] The advantage of AIE-based FL sensing is to switch on FL emission accompanied via self-assembly induced by target binding. We have already reported that selective FL detection of biologically important phosphates, adenosine triphosphate (ATP) and reduced nicotinamide adenine dinucleotide phosphate (NADPH), is possible by a steep nonlinear FL increase induced by self-assembly of guanidinium-tethered tetraphenylethene (TPE-G).^[22] Indeed, this result seems to be a striking demonstration of FL translation through self-assembly, because the targeted phosphate selectively drives self-assembly of TPE-G, which leads to a specific FL increase. The most notable point is that ATP or NADPH is selectively distinguishable from their structural analogues by the inherent threshold concentration of the FL response (the FL threshold)^[22a] and the FL intensity (the signal-to-noise (S/N) ratio).^[22b] In other words, the intrinsic information integrated within the nucleotides is expressed by the unique FL threshold and S/N ratio in the self-assembly process. In addition, the FL wavelength (color) of certain fluorophores changes in response to the aggregation

[a] Dr. T. Noguchi, Dr. B. Roy, Prof. S. Shinkai
Institute for Advanced Study, Kyushu University
744 Moto-oka, Nishi-ku, Fukuoka 819-0395 (Japan)
Fax: (+81)92-805-3814
E-mail: tnoguchi@mail.cstm.kyushu-u.ac.jp
shinkai_center@mail.cstm.kyushu-u.ac.jp

[b] Dr. T. Noguchi, Dr. D. Yoshihara, Dr. Y. Tsuchiya, Dr. T. Yamamoto,
Prof. S. Shinkai
Nanotechnology Laboratory
Institute of Systems, Information Technologies
and Nanotechnologies (ISIT)
4-1 Kyudai-Shinmachi, Nishi-ku, Fukuoka 819-0388 (Japan)

[c] Prof. S. Shinkai
Department of Nanoscience
Faculty of Engineering, Sojo University
4-22-1 Ikeda, Kumamoto 860-0082 (Japan)

Supporting information for this article is available on the WWW under
<http://dx.doi.org/10.1002/chem.201404028>.

mode,^[23] so the FL wavelength is also regarded as the output of the molecular information expressed through molecular assembly. Herein, we have made a new-perspective approach toward an assembly-based FL sensory system in which the molecular information is expressed by the following three key parameters; the FL threshold, the S/N ratio, and the maximum wavelength. In order to establish this concept, we decided to elucidate the assembly-based FL sensory system for dicarboxylate sensing,^[24a] because dicarboxylates are important biomarkers and we can procure dicarboxylate derivatives with variations from chirality to different methylene spacers.^[24b–e]

Herein, we wish to report a novel assembly-based FL sensor, a guanidinium-tethered oligophenylenevinylene derivative (OPV-G, Figure 1a). This OPV-G has three unique features:

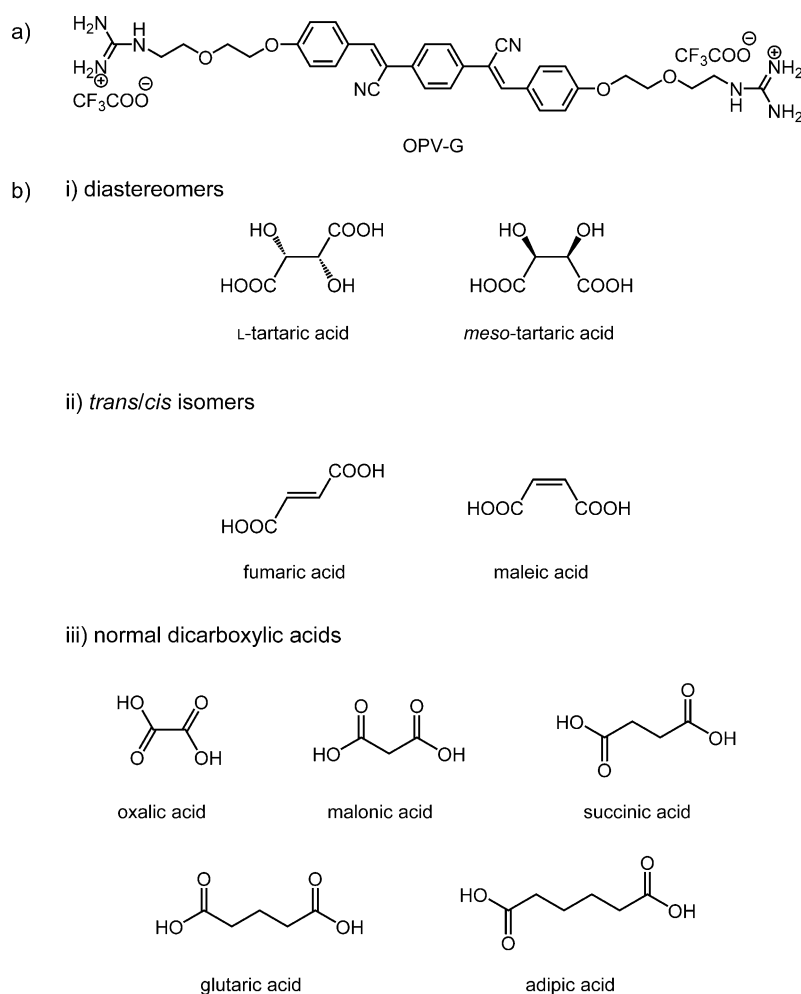


Figure 1. Chemical structures of a) assembly-based fluorescent sensor OPV-G and b) target dicarboxylic acids categorized into the three types: i) diastereomers, ii) *trans/cis* isomers, and iii) normal dicarboxylic acids.

1) The OPV-based fluorophore exhibits FL emission in response to the formation of π -stacked aggregates,^[25] a mechanism that is clearly different from that of the TPE system based on rotational restriction,^[26] 2) the guanidinium groups^[27] used as recognition sites can bind with oxo anions through specific ionic hydrogen bonding even in water,^[28] and 3) the ethereal spacers

make OPV-G soluble homogeneously in water. The dicarboxylate targets used to test the selection ability of OPV-G are shown in Figure 1b and can be categorized into the following three types: i) diastereomeric L- and *meso*-tartarates, ii) *trans/cis*-isomeric fumarate and maleate, and iii) normal dicarboxylates bearing different spacer methylene numbers. The purpose of the present study is to evaluate whether a subtle difference in the molecular information such as the chirality, geometry, and charge density encoded in the molecular structure of the dicarboxylates can critically direct the self-assembly superstructures of OPV-G and lead to characteristic FL responses. This cascade can alternatively be regarded as translation of the molecular information into FL optical signals by utilizing self-assembly phenomena (Figure 2). In this study, we demonstrate

that the molecular information embodied in the dicarboxylates is translated into the characteristic FL threshold, S/N ratio, and maximum wavelength. We propose herein that a sensory system coupled with molecular assembly phenomena will actualize its potential ability to read out the dicarboxylate structural information.

Results and Discussion

Differentiation between L- and *meso*-tartarate by the FL response of OPV-G

Although OPV-G is virtually non-fluorescent, the addition of the tartarates can make it turn on, with a FL intensity observable by our naked eyes (Figure 3a, [OPV-G] = 10 μ M, [tartarate] = 5.0 mM). The FL emission maximum appeared at 518 nm with excitation at 388 nm, but a significant difference in FL intensity was observed between the tartarate isomers; the intensity for L-tartarate was 2.5-fold higher than that for *meso*-tartarate (Figure 3b). The excitation spectra showed two characteristic peaks (358 and 388 nm for the L form and 348 and 388 nm for the *meso* form) with a shoulder component (425 nm for both). These results are in good agreement with those observed in the absorption spectra (Figure S1 in the Supporting Information). This finding indicates that the FL emission undoubtedly originates from OPV-G. Particularly interesting is the finding that the relative intensity of the excitation and absorption bands at 388 nm is different between L- and

make OPV-G soluble homogeneously in water. The dicarboxylate targets used to test the selection ability of OPV-G are shown in Figure 1b and can be categorized into the following three types: i) diastereomeric L- and *meso*-tartarates, ii) *trans/cis*-isomeric fumarate and maleate, and iii) normal dicarboxylates bearing different spacer methylene numbers. The purpose of the present study is to evaluate whether a subtle difference in the molecular information such as the chirality, geometry, and charge density encoded in the molecular structure of the dicarboxylates can critically direct the self-assembly superstructures of OPV-G and lead to characteristic FL responses. This cascade can alternatively be regarded as translation of the molecular information into FL optical signals by utilizing self-assembly phenomena (Figure 2). In this study, we demonstrate

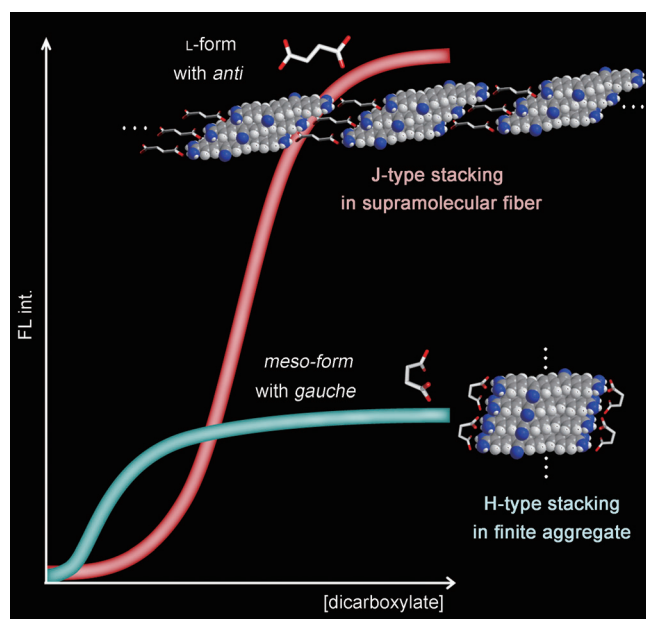


Figure 2. Schematic illustration for the concept of FL translation of L- and *meso*-tartarates through self-assembly of OPV-G.

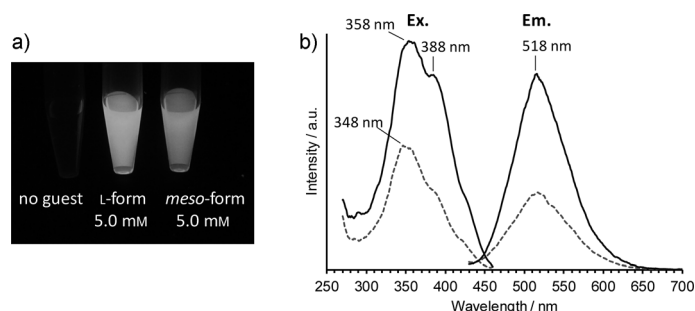


Figure 3. a) Photograph of OPV-G (10 μM) in the presence of tartarates in 2-[4-(2-hydroxyethyl)-1-piperazinyl]ethanesulfonic acid (HEPES) buffer (10 mM, pH 7.4); left: no guest; middle: L-tartarate (5.0 mM); right: *meso*-tartarate (5.0 mM). The image was obtained under UV irradiation ($\lambda_{\text{ex}} = 365 \text{ nm}$). b) Excitation ($\lambda_{\text{em}} = 518 \text{ nm}$) and fluorescence spectra ($\lambda_{\text{ex}} = 388 \text{ nm}$) of OPV-G (10 μM) in the presence of tartarates (5.0 mM) in HEPES buffer (10 mM, pH 7.4) at 25 $^{\circ}\text{C}$; solid line: L-tartarate; dotted line: *meso*-tartarate.

meso-tartarate in spite of the measurements being made under entirely the same experimental conditions. One can regard, therefore, the difference in the FL intensity as a result of the stereochemical difference between L- and *meso*-tartarate. In order to understand the FL behavior more deeply, we performed a FL titration experiment. Upon addition of L-tartarate, a FL emission increase was observed from 250 μM and its intensity reached a maximum above 1.0 mM, with the FL increase being 45-fold that in the absence of L-tartarate (Figure 4a and c). By contrast, *meso*-tartarate switched on the FL emission of OPV-G from 50 μM and the FL increase was only 18-fold at the maximum (Figure 4b and c). It is surprising that such a big difference in the FL threshold and the S/N ratio is induced by the stereochemical information of these two tartarates (Figure 4c).

One fundamental question arises: what kind of effect is operating on the FL response? An insight is found in the above-mentioned excitation and UV/Vis spectra, in which different spectral changes are observed upon addition of L- and *meso*-tartarate (Figure 3b and Figure S1 in the Supporting Information). We can address the question from the following three viewpoints: 1) the self-assembly behavior of OPV-G with L- and *meso*-tartarate, 2) the morphological studies of the aggregates formed by the self-assembly, and 3) the structural origin in the tartarates that exclusively dominates the FL emission, the self-assembly, and the morphological properties. Each factor is evaluated in the following sections.

Self-assembly behavior of OPV-G with L- and *meso*-tartarate

The UV/Vis titration of OPV-G with tartarates afforded significantly different spectral changes between the L form and the *meso* form. When the L-tartarate concentration was increased, the original absorption maximum of OPV-G at 370 nm decreased, together with a conspicuous increase in the shoulder component at 425 nm (Figure 5a). This spectral change is in good agreement with that reported in previous literature, in

which the OPV chromophores were found to be arranged in a slip-stacked fashion with respect to the direction of the molecular long axis.^[29] Herein, we classify this mode of arrangement as J-type stacking. In sharp contrast, the addition of *meso*-tartarate led to a sharp decrease in the original absorption maximum at 370 nm, together with a significant shorter wavelength shift to 344 nm in the concentration range of 0–500 μM (Figure 5b and Figure S2 in the Supporting Information). This spectral change is ascribed to H-type stacking of the OPV chromophores, as reported previously.^[25b] Although many reports have described J- or H-type aggregation in chromophoric self-assemblies,^[30–33] our results reveal a novel view that the self-assembly behaviors arising from the stereochemical difference between L- and *meso*-tartarate are clearly distinguishable according to the difference between J- and H-type aggregation. It is noteworthy that the increased concentration in the ratiometric plot of $\epsilon_{425}/\epsilon_{370}$ is also different, from

250 μM for L-tartarate and 50 μM for *meso*-tartarate (Figure 5c). The threshold concentrations of $\epsilon_{425}/\epsilon_{370}$ are indicative of the critical aggregate concentration (CAC) and, most notably, are in good agreement with those of the FL response (Figure 4c), as demonstrated in our previous report.^[22b] It is clear, therefore, that the difference in the self-assembly process (J or H type) is manifested in the characteristic FL threshold and S/N ratio.

Morphological observation of OPV-G self-assembled with L- and *meso*-tartarate

To visualize the morphologies of OPV-G self-assembled with L- and *meso*-tartarate, atomic force microscopy (AFM) was conducted for aqueous dispersion samples prepared by spin-coating on highly oriented pyrolytic graphite (HOPG). Figure 6a

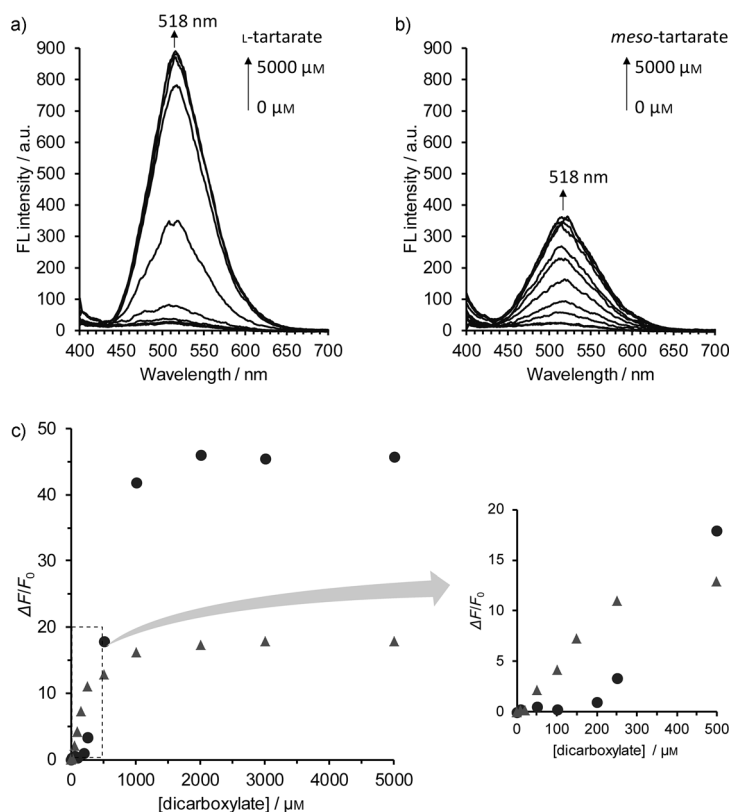


Figure 4. Fluorescence titration of OPV-G upon addition of increasing concentrations of a) L-tartarate and b) *meso*-tartarate. c) The FL titration result ($\lambda_{em} = 518$ nm; ●: L-tartarate; ▲: *meso*-tartarate) and an enlarged section of the lower concentration region (0–500 μ M). Conditions: [OPV-G] = 10 μ M, [HEPES] = 10 mM (pH 7.4), 25 °C, $\lambda_{ex} = 388$ nm. $\Delta F/F_0$ indicates the fluorescence intensity change ($\Delta F = F - F_0$, in which F is the fluorescence intensity of OPV-G at a given point and F_0 is the fluorescence intensity of OPV-G in the absence of tartarates).

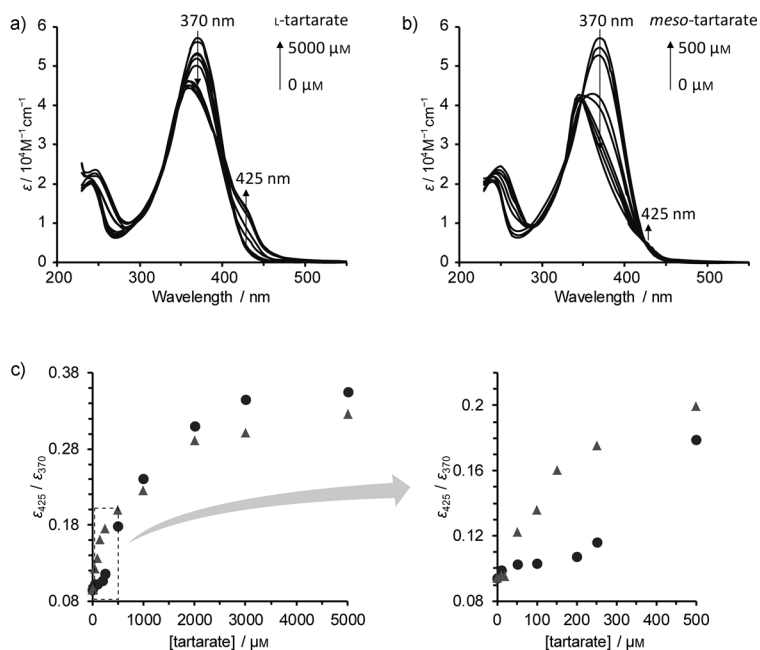


Figure 5. UV/Vis titration of OPV-G upon addition of increasing concentrations of a) L-tartarate (0–5000 μ M) and b) *meso*-tartarate (0–500 μ M for clarity). c) Ratiometric plots of $\epsilon_{425}/\epsilon_{370}$ (●: L-tartarate; ▲: *meso*-tartarate) and an enlarged section of the lower concentration region (0–500 μ M). Conditions: [OPV] = 10 μ M, [HEPES] = 10 mM (pH 7.4), 25 °C.

shows an AFM image of OPV-G J-type aggregates prepared by association with L-tartarate. One can observe well-developed fibrous superstructures of at least 35 nm in height. The formation of such a fibrous structure is supported by a J-stacking mode, as proposed by the FL microscopic observation of the aqueous dispersion (Figure S3a in the Supporting Information). In sharp contrast, an AFM image of OPV-G H-type aggregates prepared by association with *meso*-tartarate afforded a finite morphology (Figure 6b and Figure S3b in the Supporting Information) of 50–120 nm in height. Obviously, such a morphological difference stems from the difference in stereochemical information integrated in the tartarates (L form: 2*R*,3*R*; *meso* form: 2*R*,3*S*). It is surprising that the stereochemical difference of only one chiral carbon atom critically directs the self-assembled superstructure.

Structural origin in the tartarates governing the FL emission, self-assembly, and morphological properties

It has already been reported that the preferred conformations of L- and *meso*-tartarate in water are experimentally confirmed to be the *anti* and *gauche* conformers, respectively (Figure S4 in the Supporting Information).^[34] This conformational difference seems to be the origin that governs the self-assembly process leading to the characteristic FL response. In order to confirm the effect of the conformation, we employed *trans/cis*-isomeric dicarboxylates, that is, fumarate and maleate, as target molecules (Figure 1b). Unexpectedly, we found that the FL maximum wavelength is different by 6 nm. This implies that the differentiation of these isomers by FL color is possible (Figure S5a in the Supporting Information). The most important result is the finding that the FL titration of OPV-G with these regioisomeric dicarboxylates (Figure 7 and Figure S5b and c in the Supporting Information) resulted in the same tendency as that observed with the tartarates (Figure 4), which supported the idea that the preferred conformations of L- and *meso*-tartarate (*anti* and *gauche* conformations, respectively) in aqueous solution are more or less similar with those of fumarate and maleate, respectively. This result affords a clear view that the conformational difference encoded in the molecular structures can direct the course of the self-assembly. The self-assembly modes of OPV-G with L- and *meso*-tartarate are schematically illustrated in Figure 2: that is, self-assembly of OPV-G with L-tartarate (*anti* conformation) forms a supramolecular polymer with a fibrous superstructure in which the OPV chromophores are arranged in a J-type stacking manner that leads to an intense FL intensity, whereas self-assembly of OPV-G with *meso*-tartarate (*gauche*

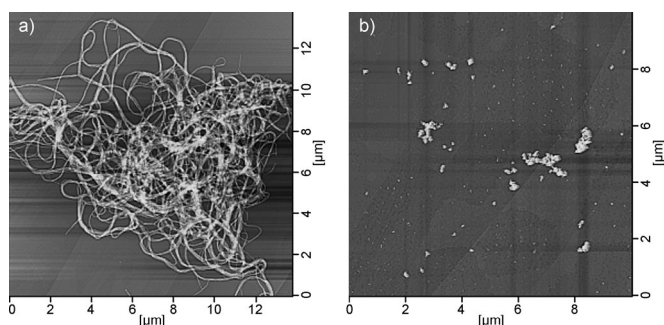


Figure 6. AFM images of OPV-G self-assembled with a) L-tartarate and b) *meso*-tartarate. Conditions: [OPV-G] = 100 μM , [tartarate] = 5.0 mM.

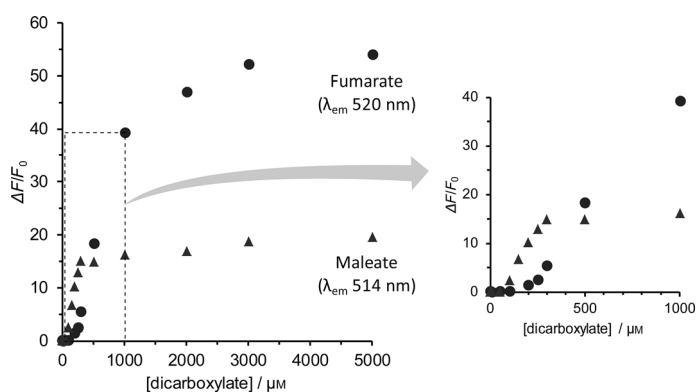


Figure 7. Fluorescence titration result of OPV-G upon addition of increasing concentrations of fumarate (●) and maleate (▲) and an enlarged section of the lower concentration region (0–1000 μM). Conditions: [OPV-G] = 10 μM , [HEPES] = 10 mM (pH 7.4), 25 $^{\circ}\text{C}$, λ_{ex} = 388 nm.

conformation) forms an H-type stacked finite aggregate that results in a modest FL intensity.

The possibility of self-assembly as an amplification tool for precise molecular recognition

From the point of view of bottom-up self-assembly, it is desirable that a small change in the molecular structure results in a dramatically different self-assembled architecture. Indeed, the present study has demonstrated that the stereochemical difference in the tartarate structures affords different self-assembled nanoarchitectures: a fibrous structure for L-tartarate and a finite aggregate for *meso*-tartarate. One may consider, therefore, that the stereochemical information about the tartarates is converted into the characteristic morphologies through self-assembly. We thus learned that such stereochemical information expressed by the characteristic self-assemblies is eventually embodied as the unique FL responses. In order to evaluate the performance level of the translation from stereochemical information to FL response through self-assembly, we tested the FL response of OPV-G toward the normal dicarboxylates illustrated in Figure 1 b. As shown in Figure 8 and Figure S6 in the Supporting Information, the FL response of OPV-G was found to exhibit a one-to-one-type relationship between

the FL titration curve and the individual molecular structures of the dicarboxylates. Namely, the molecular information about the dicarboxylates is well expressed by the characteristic FL threshold and S/N ratio. Particularly noteworthy is the clear tendency of the FL threshold and S/N ratio to increase with an increase in the methylene spacer length of the dicarboxylates. As in the case of L-tartarate and *meso*-tartarate, the FL threshold and S/N ratio are characterized by the self-assembly process of J- or H-type aggregation. Actually, a discontinuous change in the S/N ratio is observable for the FL response from malonate to succinate (Figure 8 b). This change is attributable to the formation of different types of aggregates, H type from malonate and J type from succinate, as supported by the spectral and morphological data (Figure S6 a and S7 in the Supporting Information). The shift of the FL threshold to the higher concentration is attributable to the reduced charge density (charge per molecular volume) of the dicarboxylates, which acts as the self-assembly driving force by ion pairing. In addition, the entropic factor of the longer methylene spacer might act disadvantageously, especially in the formation of fibrous superstructures, as illustrated in Figure 2. These results clearly indicate that FL translation through self-assembly is meticulous enough to sense a difference in only one carbon atom. Therefore, we wish to propose herein that self-assembly, which appears as an amplification result of the molecular structure, can be utilized as a tool for molecular recognition.

Conclusion

We have demonstrated that, by utilizing the self-assembly process of OPV-G, the structural information of dicarboxylates is successfully translated into a characteristic FL response. The FL response of OPV-G that appears through complexation with L- and *meso*-tartarate reflected the different types of self-assembly process, J and H type, with extended and finite morphologies, respectively. The chirality difference between L- and *meso*-tartarate was similarly reproduced with the geometrical difference between fumarate and maleate, respectively. As supported by the FL titration results toward normal dicarboxylates, the molecular information is definitely translated into the characteristic FL threshold, S/N ratio, and maximum wavelength characterized by the self-assembly. This FL translation is highlighted only through the self-assembly process. The utilization of self-assembly for sensory systems is going to open up a new opportunity for the design and application of a molecular sensor. We believe that it will allow a new biomedical application when an assembly-based sensor that works under physiological conditions is realized.

Acknowledgements

This work was financially supported by a Grant-in-Aid for Young Scientists (B) (grant no.: 25810051).

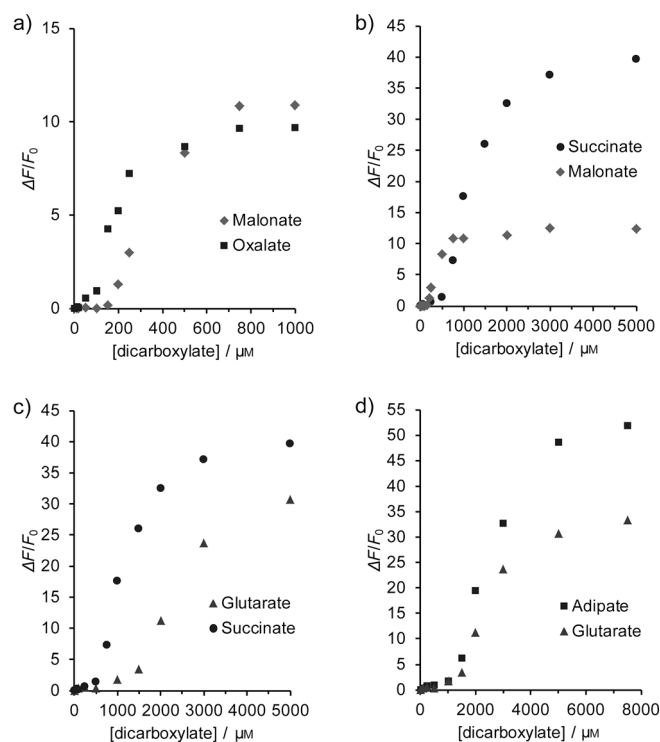


Figure 8. Comparison of the fluorescence threshold and signal-to-noise ratio: a) oxalate versus malonate, b) malonate versus succinate, c) succinate versus glutarate, and d) glutarate versus adipate. Conditions: [OPV-G] = 7.5 μM , [HEPES] = 15 mM (pH 7.4), 25 $^{\circ}\text{C}$, λ_{ex} = 388 nm.

Keywords: dicarboxylic acids · fluorescence · molecular recognition · nonlinear response · self-assembly

[1] a) J.-M. Lehn, *Supramolecular Chemistry: Concepts and Perspectives* VCH, Weinheim, **1995**; b) G. M. Whitesides, J. P. Mathias, C. T. Seto, *Science* **1991**, *254*, 1312–1319.
 [2] A. Dawn, T. Shiraki, S. Haraguchi, S. Tamaru, S. Shinkai, *Chem. Asian J.* **2011**, *6*, 266–282.
 [3] N. Kimizuka, *Adv. Polym. Sci.* **2008**, *219*, 1–26.
 [4] L. C. Palmer, S. I. Stupp, *Acc. Chem. Res.* **2008**, *41*, 1674–1684.
 [5] A. P. H. J. Schenning, E. W. Meijer, *Chem. Commun.* **2005**, 3245–3258.
 [6] T. Shimizu, M. Masuda, H. Minamikawa, *Chem. Rev.* **2005**, *105*, 1401–1443.
 [7] J. A. A. W. Elemans, R. van Hameren, R. J. M. Nolte, A. E. Rowan, *Adv. Mater.* **2006**, *18*, 1251–1266.
 [8] T. Kato, N. Mizoshita, K. Kishimoto, *Angew. Chem.* **2006**, *118*, 44–74; *Angew. Chem. Int. Ed.* **2006**, *45*, 38–68.
 [9] S. Zhang, *Nat. Biotechnol.* **2003**, *21*, 1171–1178.
 [10] M. Kasha, H. R. Rawls, M. A. El-Bayoumi, *Pure Appl. Chem.* **1965**, *11*, 371–392.
 [11] F. Würthner, T. E. Kaiser, C. R. Saha-Möller, *Angew. Chem.* **2011**, *123*, 3436–3473; *Angew. Chem. Int. Ed.* **2011**, *50*, 3376–3410.
 [12] P. D. Frischmann, K. Mahata, F. Würthner, *Chem. Soc. Rev.* **2013**, *42*, 1847–1870.

[13] F. J. M. Hoeben, P. Jonkheijm, E. W. Meijer, A. P. H. J. Schenning, *Chem. Rev.* **2005**, *105*, 1491–1546.
 [14] S. S. Babu, S. Prasanthkumar, A. Ajayaghosh, *Angew. Chem.* **2012**, *124*, 1800–1810; *Angew. Chem. Int. Ed.* **2012**, *51*, 1766–1776.
 [15] L. Maggini, D. Bonifazi, *Chem. Soc. Rev.* **2012**, *41*, 211–241.
 [16] R. Oda, I. Huc, M. Schmutz, S. J. Candau, F. C. MacKintosh, *Nature* **1999**, *399*, 566–569.
 [17] Q.-F. Sun, J. Iwasa, D. Ogawa, Y. Ishido, S. Sato, T. Ozeki, Y. Sei, K. Yamaguchi, M. Fujita, *Science* **2010**, *328*, 1144–1147.
 [18] S. Yagai, Y. Goto, X. Lin, T. Karatsu, A. Kitamura, D. Kuzuhara, H. Yamada, Y. Kikkawa, A. Saeki, S. Seki, *Angew. Chem.* **2012**, *124*, 6747–6751; *Angew. Chem. Int. Ed.* **2012**, *51*, 6643–6647.
 [19] R. Martínez-Máñez, F. Sancenón, *Chem. Rev.* **2003**, *103*, 4419–4476.
 [20] T. Noguchi, N. Kimizuka, *Chem. Commun.* **2014**, *50*, 599–601, and references therein.
 [21] Y. Hong, J. W. Y. Lam, B. Z. Tang, *Chem. Soc. Rev.* **2011**, *40*, 5361–5388.
 [22] a) T. Noguchi, T. Shiraki, A. Dawn, Y. Tsuchiya, L. T. N. Lien, T. Yamamoto, S. Shinkai, *Chem. Commun.* **2012**, *48*, 8090–8092; b) T. Noguchi, A. Dawn, D. Yoshihara, Y. Tsuchiya, T. Yamamoto, S. Shinkai, *Macromol. Rapid Commun.* **2013**, *34*, 779–784.
 [23] a) H. Tong, Y. Hong, Y. Dong, Y. Ren, M. Häußler, J. W. Y. Lam, K. S. Wong, B. Z. Tang, *J. Phys. Chem. B* **2007**, *111*, 2000–2007; b) D. Yan, A. Delori, G. O. Lloyd, T. Friščić, G. M. Day, W. Jones, J. Lu, M. Wei, D. G. Evans, X. Duan, *Angew. Chem.* **2011**, *123*, 12691–12694; *Angew. Chem. Int. Ed.* **2011**, *50*, 12483–12486.
 [24] a) T. Noguchi, B. Roy, D. Yoshihara, Y. Tsuchiya, T. Yamamoto, S. Shinkai, *Chem. Eur. J.* **2014**, *20*, 381–384, and references cited therein; b) J. L. Sessler, A. Andrievsky, V. Král, V. Lynch, *J. Am. Chem. Soc.* **1997**, *119*, 9385–9392; c) S. L. Wiskur, P. N. Floriano, E. V. Anslyn, J. T. McDevitt, *Angew. Chem.* **2003**, *115*, 2116–2118; *Angew. Chem. Int. Ed.* **2003**, *42*, 2070–2072; d) F. Han, L. Chi, X. Liang, S. Ji, S. Liu, F. Zhou, Y. Wu, K. Han, J. Zhao, T. D. James, *J. Org. Chem.* **2009**, *74*, 1333–1336; e) D. Yoshihara, Y. Tsuchiya, T. Noguchi, T. Yamamoto, A. Dawn, S. Shinkai, *Chem. Eur. J.* **2013**, *19*, 15485–15488.
 [25] a) W.-S. Xia, R. H. Schmehl, C.-J. Li, *J. Am. Chem. Soc.* **1999**, *121*, 5599–5600; b) S.-J. Yoon, J. W. Chung, J. Gierschner, K. S. Kim, M.-G. Choi, D. Kim, S. Y. Park, *J. Am. Chem. Soc.* **2010**, *132*, 13675–13683.
 [26] G. Liang, J. W. Y. Lam, W. Qin, J. Li, N. Xie, B. Z. Tang, *Chem. Commun.* **2014**, *50*, 1725–1727.
 [27] K. A. Schug, W. Lindner, *Chem. Rev.* **2005**, *105*, 67–113.
 [28] T. H. Rehm, C. Schmuck, *Chem. Soc. Rev.* **2010**, *39*, 3597–3611.
 [29] S.-J. Yoon, S. Y. Park, *J. Mater. Chem.* **2011**, *21*, 8338–8346.
 [30] a) B.-K. An, S.-K. Kwon, S.-D. Jung, S. Y. Park, *J. Am. Chem. Soc.* **2002**, *124*, 14410–14415; b) B.-K. An, D.-S. Lee, J.-S. Lee, Y.-S. Park, H.-S. Song, S. Y. Park, *J. Am. Chem. Soc.* **2004**, *126*, 10232–10233.
 [31] a) D. Oelkrug, A. Tompert, J. Gierschner, H.-J. Egelhaaf, M. Hanack, M. Hohloch, E. Steinhuber, *J. Phys. Chem. B* **1998**, *102*, 1902–1907; b) A. Ajayaghosh, C. Vijayakumar, R. Varghese, S. J. George, *Angew. Chem.* **2006**, *118*, 470–474; *Angew. Chem. Int. Ed.* **2006**, *45*, 456–460.
 [32] M. Kumar, O. A. Ushie, S. J. George, *Chem. Eur. J.* **2014**, *20*, 5141–5148.
 [33] a) S. Yagai, T. Seki, T. Karatsu, A. Kitamura, F. Würthner, *Angew. Chem.* **2008**, *120*, 3415–3419; *Angew. Chem. Int. Ed.* **2008**, *47*, 3367–3371; b) P. K. Sukul, D. Asthana, P. Mukhopadhyay, D. Summa, L. Muccioli, C. Zannoni, D. Beljonne, A. E. Rowan, S. Malik, *Chem. Commun.* **2011**, *47*, 11858–11860.
 [34] J. Ascenso, V. M. S. Gil, *Can. J. Chem.* **1980**, *58*, 1376–1379.

Received: June 19, 2014

Published online on September 18, 2014